PHOTOELASTIC FRINGE PATTERN ANALYSIS BY IMAGE PROCESSING

Antonio Francisco Gentil Ferreira Junior
Optics Laboratory, Institute for Technological Research – IPT
Av Prof. de Almeida Prado, 532 , São Paulo, 05508-901, Brazil
(agentil@ipt.br)

Oswaldo Horikawa
Department of Mechatronics Engineering, Escola Politécnica of São Paulo University
Av. Prof. Mello Moraes, 2231, São Paulo, 05508-000, SP, Brazil
(ohorikaw@usp.br)

Abstract. *This work presents a strategy for automatic analysis of photoelastic fringe patterns. The study is focused on the analysis of color type photoelastic fringes. By capturing and analyzing color fringes automatically, the difference between principal stresses of a sample are quantitatively determined. Among many techniques available in literature, the color photoelasticity is chosen as the basis for the strategy since it minimazes the operator's intervention. One important part of this technique is the calibration process, i.e., a process in which parameters of the relation between the fringe order and the fringe color are determined. This work presents a calibration based on two different filtering processes: average and harmonic. Using an experimental setup composed by a polariscope, a load system and a CCD type camera, the developed strategy is evaluated. Results of experiments are compared with the analytical solution of a disc under diametric compression for both calibration filtering processes. Despite some deviations, related to the material used in the sample and non-uniformity in the applied load, the proposed strategy showed to be efficient to evaluate the fringe order in a range of 0.5 to 3.0.*

Keywords*: photoelasticity, stress measurement, image analysis, isochromatic fringes*

1. Introduction

The photoelasticity is a method for the measurement and the experimental analysis of stress in materials. This optical method uses the temporary birefringence property (Frocht, 1941) of some transparent non-crystalline materials. Such materials are optically isotropic when free from stresses caused, for example, by external loads and become anisotropic, when an external load is applied, showing properties similar to that of crystals. This phenomenon is described by the Optical Stress Law (Frocht, 1941;Dally and Riley, 1991) and, in the case of a flat sample of constant thickness:

$$\Delta\sigma = \frac{Nf_\sigma}{h} \tag{1}$$

Where: $\Delta\sigma$ = difference between principal stress at the point;
h = thickness of the loaded sample;
N = fringe order;
f_σ = fringe value of the material, a property of the material used to prepare the sample and it depends on the wavelength of the light.

A photoelastic fringe corresponds to a region of the interference pattern where the luminous intensity is constant (usually null). This interference pattern occurs cyclically and, in a same patter, many dark fringes can be observed (see example in Fig.3(b)). The fringe order is related to the value of the phase difference of the light. Therefore, when the order of a fringe is one, the phase difference is of one wavelength.

Stress analysis can be executed by a sample made of transparent materials like acryl. The sample is loaded and then, the stress analyzed by analyzing the photoelastic fringe pattern.

A noticeable development was observed in photoelasticity technique in the last decades, during which, the digital image processing techniques was introduced for interpreting automatically the measurement results. In the past, this process was strongly dependent of the experience and the skill of the system user.

The first systems for digital processing of photoelasticity images was developed around the 70's and executed simple image processing such as thinning of lines (Müller and Saakel, 1979; Seguchi, Tomita and Watanabe, 1979). The real potential of the digital image processing became evident when fringe patterns were considered as a phase map. In this new approach, a fringe order is associated to each pixel of an image.

The half-fringe photoelasticity (Voloshin and Burger, 1983) determines the fringe order in a monochromatic image by analyzing the grayscale intensity of each pixel. However, due to the periodicity of the fringe pattern, the determination of the absolute order of a fringe can be made for values from 0 to 0.5 fringe orders. This limitation affects directly the range of difference between principal stresses that can be measured.

The phase-shift technique (Hecker and Morche, 1986; Patterson and Wang, 1991; Chen and Lin, 1998) expands the range of the fringe order measurement. However, the obtained result requires a complementary technique to determine the absolute value of the fringe order. Despite the limitation, this technique can determine the direction of principal stress as well as, the difference between stresses. Principal stresses can be determined by the stress separation technique (Frocht, 1941; Dally and Riley, 1991).

The RGB photoelasticity (Ajovalasit, Barone and Petrucci, 1995; Ramesh and Deshmukh, 1996) determines the fringe order by the color of the fringe pattern, enabling the measurement of the absolute fringe order in the interval of 0.5 to 3. Direction of principal stresses can be determined by modifying the technique (Yoneyama et al, 1998).

In this context, this work presents a strategy for automatic analysis of photoelastic isochromatic fringe, aiming quantitative evaluation of the difference between principal stresses. The above mentioned, RGB photoelasticity, is selected as the basis of the strategy, because it offers more possibilities for a high level of automation in the fringe evaluation process. The strategy to be developed is able of: analyzing the isochromatic fringe pattern, determining the order of each fringe and then, determining the difference between principal stresses.

2. The analysis strategy

Figure 1 shows the setup to be considered to obtain photoelasticity images. White light, uniformly provided by an illumination device, is linearly polarized by the first polarizer (PL) and circularly polarized by the first quarter wave plate (QL). After passing through the sample (an acryl made disc is used in experiments), the light is linearly polarized by the second quarter wave plate (QR) and pass through the second polarizer (PR), that creates dark or brightness regions, i.e., the fringe pattern. The polarization axis of PL is set orthogonal to the PR in order to obtain a dark background in the fringe patterns. The fringe pattern, is then captured by a CCD camera and sent to a computer, that executes the automatic analysis, according to the proposed strategy.

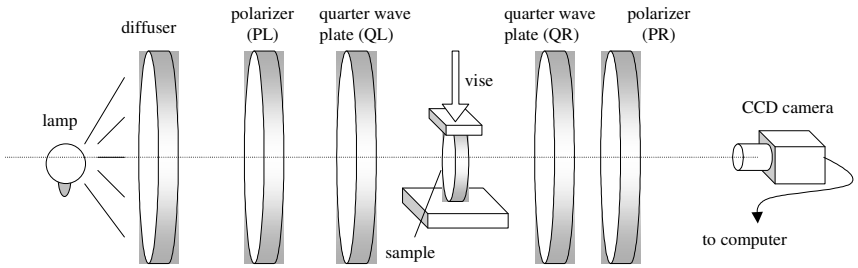

Figure 1. Schematics of the setup for analysis by photoelasticity.

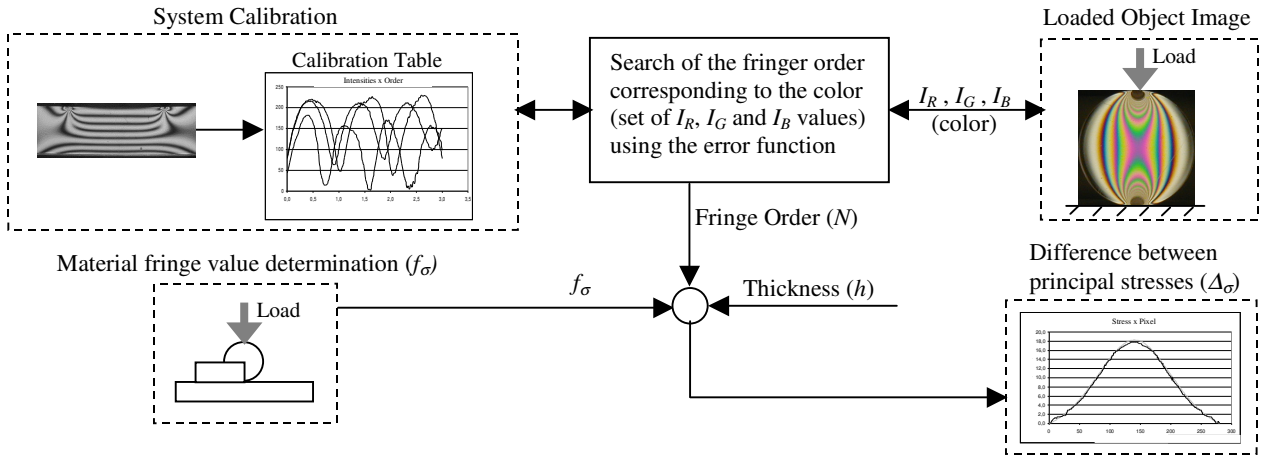

Figure 2. Schematics of the strategy for isochromatic fringe analysis.

Figure 2 presents schematics of the strategy of analysis, showing the main activities to be executed. The strategy is developed based on works concerning RGB photoelasticity (Ajovalasit, Barone and Petrucci, 1995; Ramesh and Deshmukh, 1996). It is divided into three parts: (1) calibration of the image processing system, (2) measurement of the fringe value of the material and (3) determination of the fringe order.

2.1. Calibration of the image processing system

The calibration of the fringe analysis system becomes necessary since the intensity of the light coming from a fringe pattern depends on: the type of material used to construct the sample, the light coming from the polariscope and the sensibility of the CCD camera (Redner, 1985). The calibration is exclusive for that setup. If, at least, one component of the setup is replaced, the calibration should be executed again.

The calibration consists of obtaining a correlation between each fringe order and the corresponding intensity of each RGB (red, green and blue) color component of a fringe pattern. A monochromatic image and a color image are required for the calibration. The monochromatic image provides the variation of the fringe order according to the pixel position. The color image provides the absolute value of the fringe order and the corresponding color, i.e., set of intensities in terms of RGB components for each pixel position. In this work, the calibration is made using a photoelastic pattern obtained using a beam with rectangular cross section, loaded at two positions, as shown in Fig.3(a). A loaded beam gives a fringe patterns in which, the fringe order varies linearly according to the position in the model. Therefore, the relation between the fringe order and the pixels position is linear.

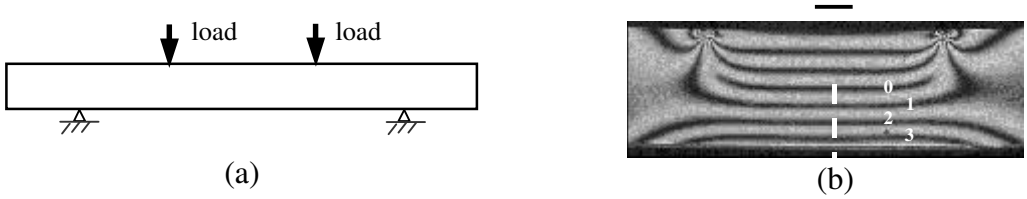

Figure 3. (a) A beam loaded. (b) Photoelastic fringe pattern obtained by monochromatic light (575nm).

The fringe order is determined from the variation of the pixel intensity along the dashed line of Fig. 3(b). With the fringe order and the respective pixel position, the linearity is evaluated by using a linear regression, as indicated in Fig.4.

Once, the linearity of the relation between pixel position and the fringe order, is verified, the next step consists of obtaining the calibration table, i.e., the relation between fringe order and the RGB intensity. The calibration is executed using the relation shown in Fig.4 and the color image of the Fig.3(b).

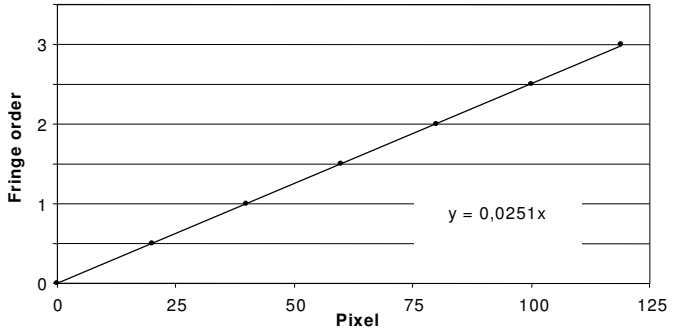

Figure 4. Relation between pixel position and fringe order.

RGB intensity of each pixel of the color image is captured adopting as the reference, the position of the zero order fringe that can be found in the monochromatic and in the color image. To reduce the noise present in the RGB intensities two solutions are proposed: an averaging filter and a harmonic filter applied to RGB intensities. The average filter is a 1×100 matrix containing the value 1/100 in each element. This filter was applied to the pixels along the dashed line of the Fig.3(b). The size of the filter is indicated by the solid line in the top of the Fig.3(b). The harmonic filter selects the 10th first harmonics of the RGB intensities obtained by the average filter. The filtered relations between fringe order and values of intensity of R, G and B planes are shown in Fig.5.

The remaining noise, still present in the intensities (Fig.5) is caused by oscillation in the image acquisition system, by scratches, by non-homogeneities of the material used to construct the model and in the illumination.

Images are obtained by digital camera under the resolution of 1280×960 pixels and stored without compression. The camera is a 1/2.7 inch size CCD type camera with 1.3M pixels.

2.2. Measurement of the fringe (f_σ) value of the material

The fringe value is a property that depends on the material used to prepare the photoelastic model. This can be determined by the procedure described by Dally and Riley (1991). The procedure is based on the use of the following analytical solution for principal stresses of a diametrically loaded disc (Frocht, 1941).

$$\Delta\sigma = \frac{8P}{\pi hD}\left[\frac{D^4 - 4D^2x^2}{\left(D^2 + 4x^2\right)^2}\right] \tag{2}$$

Where: $\Delta\sigma$ = difference between principal stresses
P = the applied load
h = the thickness
D = the diameter
x = the distance, from the center of the disc

Firstly, parameters P, h and D are defined. Then, using Eqs.(1) and (2) and counting the fringe order (N) at the center of the disc (counted manually, considering that N=0 at the border), the fringe value of the material is determined. Fig.6 presents the setup used to determine the fringe value. A vice applies a known load on the sample, an acryl made disc. A block gauge, located in front of the disc, gives the position of the center of the disc in the fringe pattern. As the load is varied, the fringe order at the center is counted. This gives an experimental linear curve that correlates the applied load to the corresponding fringe order at the center. Therefore, its inclination gives the fringe value.

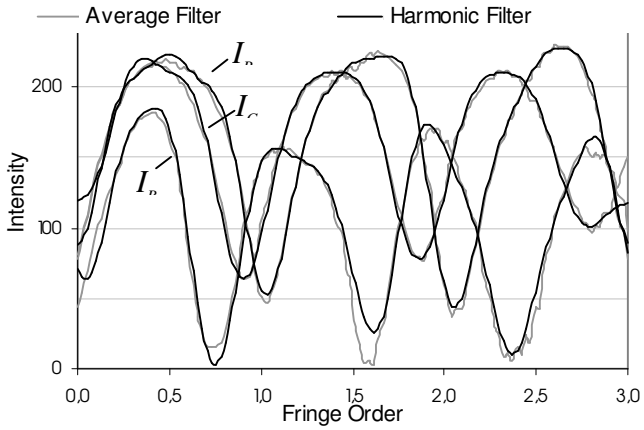

Figure 5. Calibration tables using the average filter and the harmonic filter.

The fringe value of the material is determined while the disc is loaded and unloaded. Tab.1 presents measured fringe values. Considering the uncertainties, both results coincide well. During the unloading, a slice upward shifting is observed in the curve of fringe value, when compared to that obtained during the loading. This is caused by residual stress that remained in the acryl sample during the unloading. However, this does not affect the fringe order determination.

Table 1. Obtained fringe value of the material.

	f_σ (N/order/mm)[(1)]
Load	135,6 ± 3,4
Unload	146,4 ± 9,0

[(1)]: The unit for f_σ is Newton per finger order per millimeter.

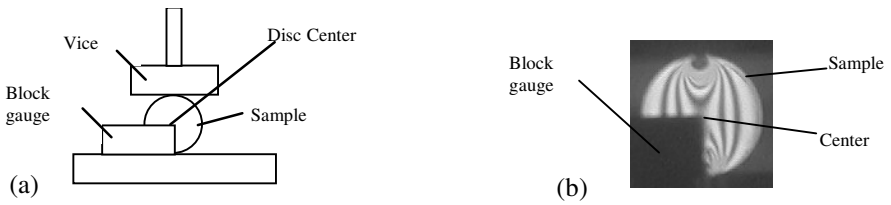

Figure 6. (a) Setup for determining the fringe value. (b) Obtained image.

2.2. Determination of the fringe order

The fringe order identification process is executed for each pixel of an image corresponding to a photoelastic pattern, using intensity values at the R, G and B planes (respectively, I_R, I_G and I_B). These intensities are compared to a set of intensities obtained in the calibration process (I_{Rc}, I_{Gc} and I_{Bc}). Using an error function (E), described below, the experimentally obtained set of RGB intensities is compared to the set of intensity values for each fringe order in the calibration curve. The fringe order of the calibration table that gives the smallest error is chosen as the fringe order at that pixel.

$$E = (I_R - I_{Rc})^2 + (I_G - I_{Gc})^2 + (I_B - I_{Bc})^2 \tag{3}$$

3. Measurement results

In order to evaluate the strategy, presented in this work, the same analytical model presented by Eq.(2) is considered. Different of the model used in the calibration, in the diametrically loaded disc, the relation between fringe order and the pixel position is non-linear. The difference between principal stresses at the horizontal diametrical line of the disc is determined analytically and experimentally by the presented strategy and both results are compared. The disc used in experiments has a diameter of 14.81±0,02mm and loaded by a 2490±51N force. Images are captured under the resolution of 0.055mm/pixel. The disc was loaded and the Fig.7(a), obtained. Then, the disc was unloaded and loaded again, obtaining the Fig.7(b). Fig.7(a) is analyzed first.

Figure 7. Fringe patterns acquired by the CCD camera. (a) First loading. (b) Second loading.

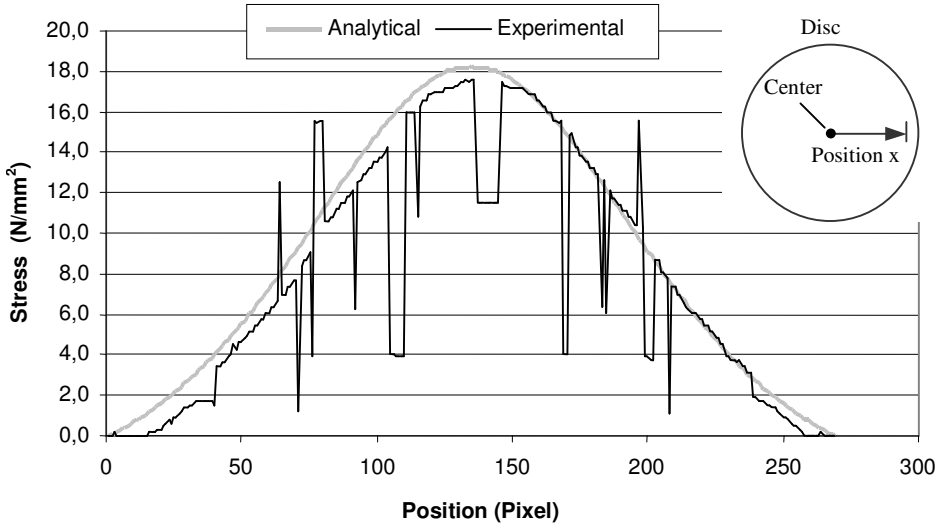

Figure 8. Difference between principal stresses using average filter calibration.

Results of comparison for both calibration types are presented in Figs.8 and 9. Errors in the fringe order determination are observed in several parts of the graphs. As already explained, the error function identifies the fringe order based on the comparison of the RGB intensities in each pixel with the RGB intensities given by the calibration table. Errors verified in the results by the average filter (Fig.8) are due to oscillation in the image acquisition system, scratches in the sample, non-homogeneities in the material used to prepare the sample and non-homogeneities in the illumination. Theses errors occur both, at the setup calibration and during the experiments. Another source of error is the similarity of RGB calibration intensities which have intensities of (204;169;27) and (205;201;24) for fringe orders of 0.68 and 2.45, respectively. The error verified in the results by the harmonic filter (Fig.9) are caused by the same

error components of the previous. In addition, here, an error arises from the divergence between the curve fitted by harmonic filter and the original curve for low and high finger orders.

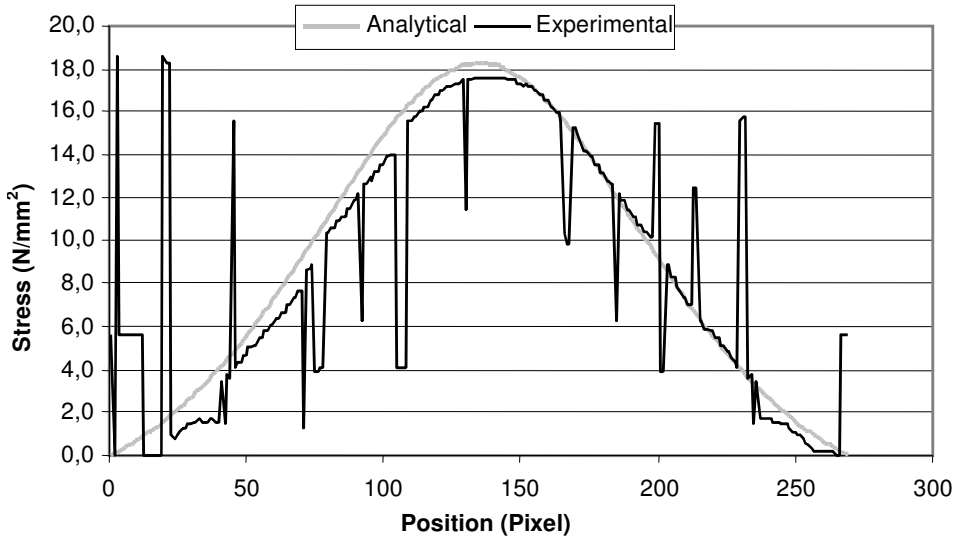

Figure 9. Difference between principal stresses using the harmonic filter calibration.

4. Discussion

Experimental results are affected by the noise existing in the RGB intensities. Ramesh and Deshmukh (1996), developed an searching algorithm that eliminates the noise. In the algorithm, the fringe order of a pixel is compared to the fringe order of the previous pixel. If the difference of fringe order is among ±0.25 order, the value is stored and the algorithm processes the next pixel. If not, the algorithm searches for fringe order that gives the next minimum of the error function. This process is repeated until the condition for the fringe order is satisfied.

A similar algorithm is developed in this work. The developed algorithm adopts a tolerance range of ±0.3 order and searches up to 10 times for the minimum of the error function. If an acceptable value is not found during 10 searches, the result will be null. The result obtained by this algorithm is presented in Fig.10 for the average calibration.

This modification in the algorithm is not efficient in the case of harmonic calibration because of errors for low fringe order values, as shown in Fig.9. These errors are consequence of the lack of high order harmonics in the original set of RGB intensity values, used in the calibration, affecting the first interaction of the algorithm, which stars with a reference fringe order equal to zero.

The developed algorithm reduces the effects of the noise present in the calibration table and the image obtained from the sample. Effects of noises are significantly removed in the experimental result showing the effectiveness of the proposed strategy.

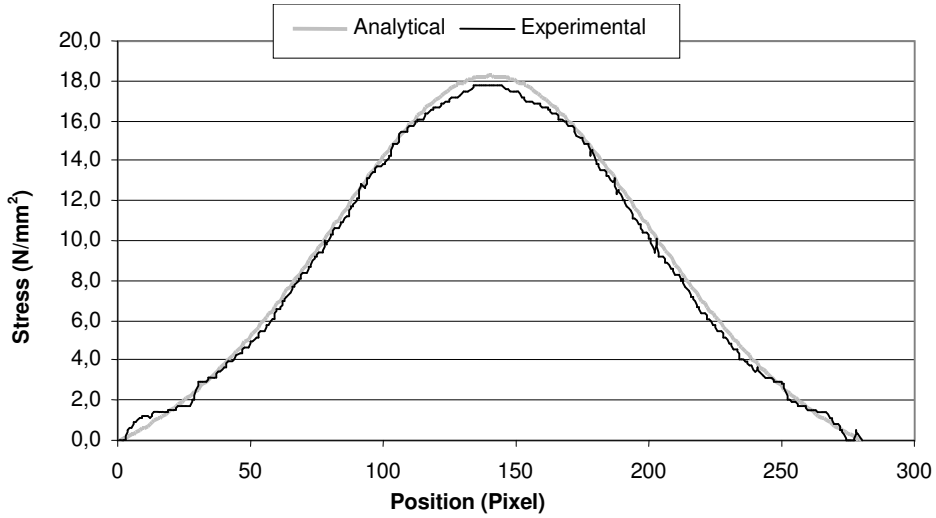

Figure 10. Difference between principal stresses using the average filter calibration (2nd loading).

In Figs. 8 and 9, experimental curves are shifted to the right when compared to the analytical curve. This is caused by non-uniformity in the load applied to the disc as can be observed by dark regions indicated by circles, in the superior and inferior parts of the fringe pattern (Fig.7(a)). These dark regions are tilted to the right direction, indicating that the

load is not applied orthogonally. Thus, in the experiments, the center of the loading does not coincides with the disc center while the analytical result was obtained assuming that both centers coincide.

The shifting of the experimental curve downward (Fig.10), with respect to the analytical curve, is a consequence of an error in the fringe value measured from the material and residual tensions that remained in the acryl.

A discontinuity occurs in the interval of 2 to 3 N/mm^2 (0.3 to 0.5 order) in Figs. 8 and 9. Fringe orders are not accurately determined in this interval. This occurs because the RGB intensities are almost constant in the calibrations. This represents a limitation on determining the fringe order inferior to 0.5 order.

The fringe order determination is limited to 3.0 order, since, for larger fringe orders, RGB intensities converge to constant values, i.e., colors of the fringes become weak, making difficult the fringe identification. Ajovalasit, Barone and Petrucci (1995) as well as Ramesh and Deshmukh (1996) reported similar effect in their works.

Until here, all analysis was conducted concerning Fig.7(a). Fig.7(b) shows the repeatability of the measurement by the image processing system and confirm the effect of the non-uniformity of the loading, the disc is loaded again. The uniformity of the fringe pattern is better than that observed in Fig.7(a). The analysis of this image (Fig.10) shows that the lateral shifting of the experimental curve with respect to the analytical curve is almost null.

5. Conclusions

This work presented a image processing system for automatic analysis of photoelastic isochromatic fringes used for quantitative evaluation of the difference between principal stresses. The system considers a photoelastic analysis system composed of a polariscope, a load system, a CCD camera and a computer. The fringe order is automatically identified based on the RGB photoelasticity technique.

Experimental values of difference between principal stresses, obtained by the presented strategy, are compared to analytical ones. The comparison showed the efficiency of the system to interpret photoelastic isochromatic fringes automatically, making possible the quantitative evaluation of difference between principal tensions. A computational algorithm for fringe analysis is developed so as to be capable of reducing errors consequent of noises present in the images. Better results for error correction are achieved using average filter calibration than harmonic filter. Some deviations remained in results due to non-uniformity in the loading, during experiments. The system gives a measurement range of 0.5 to 3 fringe orders.

The image processing system can be improved so as to measure values of principal tensions. This will require an additional processing module that identifies directions of the principal tensions. It will be theme for future works.

6. References

Ajovalasit, A., Barone, S. and Petrucci, G., 1995, “Towards RGB Photoelasticity: Full-field Automated Photoelasticity in White Light”, Experimental Mechanics, Vol.35, No.3, pp.193-200.

Chen, T.Y. and Lin, C.H., 1998, “Whole-field Digital Measurements of Principal Stress Directions in Photoelasticity”, Optics and Lasers in Engineering, Vol.30, pp.527-537.

Dally, J. W. and Riley, W. F., 1991, “Experimental Stress Analysis”, McGraw-Hill, New York, 3rd ed..

Frocht, M. M., 1941, “Photoelasticity “, John Wiley & Sons, New York, Vol.1.

Hecker, F.W. and Morche, B., 1986, “Computer-aided Measurement of Relative Retardations in Plane Photoelasticity”, In: WIERINGA, H. editor. Experimental Stress Analysis. The Netherlands: Martinus Nijhoff Publishers, pp.535-542.

Müller, R. K. and Saackel, L. R., 1979, “Complete Automatic Analysis of Photoelastic Fringes”., Experimental Mechanics, Vol.19, n.7, pp.245-251.

Patterson, E.A. and Wang, Z.F., 1991, “Towards Full Field Automated Photoelastic Analysis of Complex Components”, Strain, Vol.27, No.2, pp.49-56.

Ramesh, K. and Deshmukh, S.S., 1996, “Three Fringe Photoelasticity - use of Colour Image Processing Hardware to Automate Ordering of Isochromatics”, Strain, Vol.32, No.3, pp.79-86.

Redner, A.S., 1985, “Photoelastic Measurements by Means of Computer-Assisted Spectral-Contents Analysis”, Experimental Mechanics, Vol.25, No.2, pp.148-153.

Seguchi. Y., Tomita, Y. and Watanabe, M., 1979, “Computer-aided Fringe-pattern Analyzer – A Case of Photoelastic Fringe”, Experimental Mechanics, Vol.19, No.10, pp.362-370.

Voloshin, A.S. and Burger, C.P., 1983, “Half-fringe Photoelasticity: A New Approach to Whole-field Stress Analysis”, Experimental Mechanics, Vol.23, No.9, pp.304-313.

Yoneyama, S. et al. Photoelastic, 1998, “Analysis with a Single Tricolor Image”, Optics and Lasers in Engineering, Vol.29, pp.423-435.

7. Responsibility notice

The authors are the only responsible for the printed material included in this paper.